

# Cornea in Marfan Disease: Orbscan and In Vivo Confocal Microscopy Analysis

Gilles Sultan,<sup>1,2</sup> Christophe Baudouin,<sup>1,2</sup> Olivier Auzerie,<sup>1,2</sup> Magdalena De Saint Jean,<sup>1,2</sup> Marie Goldschild,<sup>1</sup> the Marfan Study Group, and Pierre-Jean Pisella<sup>1,3</sup>

**PURPOSE.** To investigate corneal thickness, curvature, and morphology with the Orbscan Topography System I (Bausch & Lomb, Inc., Salt Lake City, UT) in patients with Marfan syndrome (MFS) and to study MFS with in vivo confocal microscopy.

**METHODS.** This prospective, clinical, comparative case series included 60 eyes of 31 patients with MFS and 32 eyes of 17 control subjects. First, biomicroscopic examination was conducted to search for ectopia lentis. Then, mean keratometry and ocular refractive power were calculated by the autokeratorefractometer. In each group, the Orbscan System I mean (and mean simulated) keratometry and pachymetric measurements (at the central location and at eight midperipheral locations) were obtained and compared, and correlations were established. In vivo confocal microscopy was performed to evaluate tissue morphology and Z-scan analysis of 14 thin MFS corneas compared with 14 control corneas.

**RESULTS.** A significant decrease (ANOVA,  $P < 0.0001$ ) of mean simulated keratometry measurement appeared in the MFS group (sim K,  $40.8 \pm 1.4$  D) compared with the control group ( $42.9 \pm 1.1$  D). Pachymetry in the MFS group was significantly decreased ( $P < 0.0001$ ) compared with that in the control group, in the center (respectively,  $502 \pm 41.9$   $\mu\text{m}$  and  $552 \pm 23.6$   $\mu\text{m}$ ) and the eight midperipheral locations. Ectopia lentis was highly linked with mean keratometry and pachymetry ( $P < 0.0001$ ). Confocal microscopy performed on MFS-affected thin corneas confirmed the corneal thinning and showed an opaque stromal matrix, and Z-scan profiles were abnormal with increased stromal back scattering of light.

**CONCLUSIONS.** MFS is known to be associated with a flattened cornea. This study demonstrated an association with corneal thinning and described confocal microscopy findings in this syndrome. (*Invest Ophthalmol Vis Sci.* 2002;43:1757-1764)

Marfan syndrome (MFS) is an autosomal dominant disorder of connective tissues, with an incidence of 1:10,000. It does not appear as an isolated entity, but as a common disorder in a continuous clinical spectrum of overlapping phenotypes: the type 1 fibrillinopathies.

From the <sup>1</sup>Department of Ophthalmology, Ambroise Pare Hospital, University of Paris-V, Paris, France; the <sup>2</sup>Department of Ophthalmology III, Quinze-Vingts Hospital, Paris, France; and the <sup>3</sup>Department of Ophthalmology, University Hospital Center (CHU) Bretonneau, Tours, France.

Presented in part at the annual meeting of the Association for Research and Vision in Ophthalmology, Fort-Lauderdale, Florida, May 2001.

Submitted for publication June 26, 2001; revised December 3, 2001; accepted December 14, 2001.

Commercial relationships policy: N.

The publication costs of this article were defrayed in part by page charge payment. This article must therefore be marked "advertisement" in accordance with 18 U.S.C. §1734 solely to indicate this fact.

Corresponding author: Christophe Baudouin, Quinze-Vingts Hospital, Ophthalmology III Dept, 28 rue de Charenton, 75012 Paris, France; arepo@worldnet.fr.

Fibrillin-1, a 350-kDa acidic glycoprotein, is encoded by the fibrillin gene (*FBNI*) located on chromosome 15q15-21,<sup>1-4</sup> and is a major component of the 10- to 12-nm extracellular microfibrils. It is known to play a critical role in the strength and elasticity of ocular connective tissues.

MFS is characterized by pleiotropic manifestations primarily involving the optical, skeletal, and cardiovascular systems. A spectrum of ocular abnormalities are associated with MFS, including retinal detachment, increased axial length and myopia, flattened cornea, iris and ciliary muscle hypoplasia, and ectopia lentis.<sup>5</sup> In many cases, ectopia lentis is difficult to detect, thus diagnosis is often uncertain. It is important to note that complications of MFS may be serious and that visual and vital functions can be affected. For this reason, a new ocular sign directly correlated with ectopia lentis would greatly facilitate diagnosis, which is often very difficult to validate. The purpose of our study was to evaluate the corneal thickness in MFS with the aid of the Orbscan Corneal Topography System I (Bausch & Lomb, Inc., Salt Lake City, UT), an optical scanning slit instrument that measures corneal thickness at any point on the cornea with precision and accuracy,<sup>6,7</sup> and to describe confocal microscopy findings in this syndrome.

## METHODS

### Study Design

Between June and October 2000, 60 eyes (30 right and 30 left) of 31 patients with MFS were compared with 32 eyes (17 right and 15 left) of 17 patients of a control group. The MFS group was composed of 17 (54.8%) males and 14 (45.2%) females. There were 28 (90.3%) white subjects and 3 (9.7%) subjects belonging to other ethnic groups. The control group was composed of 9 (52.9%) males and 8 (47.1%) females, with 15 (88.2%) white and 2 (11.8%) nonwhite subjects.

Patients were referred to the Marfan Clinic, at Ambroise Pare Hospital, Paris-V University (Boulogne, France) where five specialists (a geneticist, a pediatrician, a rheumatologist, an ophthalmologist, and a cardiologist) examined them successively on the same day. Sixty-five percent of them were attending for primary consultation and the others for follow-up consultations. In our study, every patient with MFS had a positive diagnosis, according to the Berlin criteria.<sup>5</sup> In difficult patients, two genetic tests were used: first, evaluation of fibrillin production in a skin biopsy specimen, for diagnosis of type-I fibrillinopathy; and second, a molecular test allowing identification of a mutation in the *FBNI* gene or cosegregation of a polymorphic genetic marker within the *FBNI* gene, in all families. Despite all these criteria, diagnosis remained uncertain in 11% of all patients after multidisciplinary consultation. None of these patients was included in the two groups. Moreover, it is important to note that our control group was composed of patients who had an absolutely negative MFS diagnosis, but who were referred to our clinic for confirmation or rejection of the diagnosis. Therefore, they often had an MFS habitus or several conditions in the medical history that resembled MFS.

In both groups, patients reported no history of contact lens use, refractive surgery, ocular irritation, corneal edema or disease. Two patients who wore soft contact lenses were asked to remove them 2 days before the scheduled appointment.

## Procedures

For each patient, the procedure was fully explained, and consent was obtained, according to the ethics committee of Ambroise Pare Hospital (University Paris-V), and in adherence to the Declaration of Helsinki for research involving human subjects. Our ophthalmic investigations were based on the Berlin criteria.<sup>5</sup> First, the three minor abnormalities in favor of the presence of MFS were sought. In this way, a systematic interrogatory was performed to search for a retinal detachment antecedent, and a noncontact fundus examination was performed. Then, the mean K measurement and the ocular refractive power were established by the autokeratorefractometer (model KR.3500; Topcon Inc, Paramus, NJ); ametropia was evaluated with the spherical equivalent.

Second, ectopia lentis, a major sign according to the Berlin criteria, was systematically sought by biomicroscopic examination, with complete pupillary dilation and with different positions of the eye, and was classified according to its severity and location (inferior, superior, superonasal, or superotemporal).

## Orbscan Analysis

The Orbscan Corneal Topography System I (Bausch & Lomb, Inc., Salt Lake City, UT) was used in this study (hardware essentially composed of a computer system with a Pentium processor [Intel Corp., Santa Clara, CA] and Windows NT operating system [Microsoft Corp., Redmond, WA]). Accuracy and variability (precision) of pachymetry measurements using the Orbscan system were shown elsewhere to be acceptable for research use.<sup>6</sup> Examinations were always performed by the same practitioner to capture all data in the same manner and at the same time of day for all procedures. Indeed, according to a prior study, early morning Orbscan central and peripheral pachymetries seemed to be highly variable,<sup>6</sup> with a diurnally based hydration gradient across the peripheral cornea.

The Orbscan System I software, Orbtex (Bausch & Lomb, Inc.), calculated many data in the cornea. In the two groups, we measured mean keratometry in the 3.0-mm central zone (mean K), the mean simulated keratometry (sim K), the mean astigmatism in the 3.0-mm central zone (mean A), and the mean simulated astigmatism (sim A).

Then, nine pachymetry measurements (obtained from the difference in elevation between the anterior and posterior surfaces) and location data were studied as previously described<sup>8</sup> in normal eyes. They are represented by 9 circles of 2 mm diameter each located 3 mm from the visual axis (Figure 3 shows 11 circles): the central corneal thickness, and at eight locations in the midperipheral cornea. These 9 circles are central, superotemporal, temporal, inferotemporal, inferior, inferonasal, nasal, superonasal, and superior. Moreover, the thinnest corneal point, its distance from center, and its quadrant location (superonasal, inferonasal, inferotemporal, and superotemporal) were identified by the Orbscan software and analyzed.

As previously described,<sup>8</sup> in the pachymetry maps the warmest color identifies the thinnest corneal area and designates one of four different patterns (depicted in Figure 3) namely round, oval, decentered round, and decentered oval. In the round pattern, the ratio of the shortest to the longest diameter (SD-LD) of the warmest-colored zone is greater than or equal to two thirds, and the warmest color is either entirely located at the center of the map or more than half of the area of the warmest color enters the central 3-mm diameter zone. In the

TABLE 1. Demographic Characteristics by Diagnostic Group

	MFS	P*	Control
Number of eyes	60		32
Number of patients	31		17
Age (y)			
Mean $\pm$ SD	23.9 $\pm$ 14.3	0.12	29.8 $\pm$ 21.4
Range	5-50		4-70
Sex (n, %)			
Male	17 (54.8)		9 (52.9)
Female	14 (45.2)		8 (47.1)
Race (n, %)			
White	28 (90.3)		15 (88.2)
Other	3 (9.7)		2 (11.8)

\* Compared with control.

oval pattern, the ratio SD-LD is less than two thirds, and the warmest color is situated the same as in the round pattern. In decentered patterns, the warmest color is either round or oval, and more than half of its area is outside the 3-mm central diameter zone or is entirely located in the peripheral cornea.

## Confocal Scanning Microscopy

In vivo confocal scanning microscopy (ConfoScan P4; Tomey, Nagoya, Japan) was performed in 14 significantly thin corneas of seven patients with MFS, and in 14 control corneas, to seek any difference between both groups. Integrity and morphologic features of the corneal stroma and endothelium in MFS were evaluated. Thickness measurements and Z-scan patterns were analyzed in both groups.

## Statistical Analyses

Results were calculated as arithmetic means  $\pm$  SD; significance was calculated by means of two-way analysis of variance (ANOVA) and Student's *t*-test, with *P* < 0.05 regarded as significant. The  $\chi^2$  test was used for qualitative comparisons. Statistical correlations were performed with the *z* correlation test, also at a 0.05 level of significance (Statview IV for Windows; Abacus, Berkeley, CA).

## RESULTS

### Clinical Findings

Demographic information and clinical aspects are summarized in Tables 1 and 2. Sixty eyes of 31 patients with MFS were compared with 32 eyes of 17 patients of a control group. Mean age in the MFS group was 23.9  $\pm$  14.3 years (range, 5-50) versus 29.8  $\pm$  21.4 years in the control group (range, 4-70; NS).

Mean K performed in the two groups with the autokeratorefractometer, was significantly lower in the MFS group (mean  $\pm$  SD, 41.4  $\pm$  1.4 D; range, 38.1-44.2) compared with the one obtained in the control group (43.0  $\pm$  1.0 D; range, 41-45, *P* < 0.0001 between both groups). In the MFS group, 32 (53.3%) of 60 eyes were statistically flattened (below 41.5 D) versus only

TABLE 2. Clinical and Autorefractometer Data

	Marfan		P*	Control	
	Mean $\pm$ SD	(Range)		Mean $\pm$ SD	(Range)
Mean K (D)	41.4 $\pm$ 1.4	(38.1-44.2)	<0.0001	43.0 $\pm$ 1.0	(41.0-45.0)
Refractive power (D)	-1.1 $\pm$ 2.2	(-8-+2)	0.06 (NS)	-0.25 $\pm$ 1.5	(-4.5-+3)
Ectopia lentis (%)	86.7		<0.0001	0	

\* Compared with control.

TABLE 3. Orbscan Corneal Topography System Data

	Marfan			Control	
	Mean $\pm$ SD	(Range)	<i>P</i> *	Mean $\pm$ SD	(Range)
Mean K (D)	40.8 $\pm$ 1.4	(37.5–43.9)	<0.0001	42.8 $\pm$ 1.0	(40.5–44.8)
Sim K (D)	40.8 $\pm$ 1.4	(37.5–43.9)	<0.0001	42.9 $\pm$ 1.1	(40.4–44.9)
Mean A (cylinder in D)	1.09 $\pm$ 0.87	(0.1–4.9)	0.06 (NS)	0.78 $\pm$ 0.47	(0.1–2.0)
Sim A (cylinder in D)	1.07 $\pm$ 0.84	(0.1–5.2)	0.03	0.72 $\pm$ 0.43	(0.1–1.7)
Central thickness ( $\mu$ m)	502.0 $\pm$ 41.9	(429–606)	<0.0001	552.4 $\pm$ 23.6	(510–609)
Thinnest corneal point ( $\mu$ m)	487.2 $\pm$ 42.2	(412–585)	<0.0001	542.2 $\pm$ 25.0	(496–598)

Mean K and mean A are in the 3.0-mm central zone.

\* Compared with control.

5 (15.6%) of 32 eyes in the control group, which was significantly higher ( $P < 0.0001$ ). Nine eyes (15%) of the MFS group had mean corneal power below 40.0 D (none in the control group), which corresponds to a considerably flattened cornea.

Ocular refractive power, measured as spherical equivalent, was not significantly different ( $P = 0.06$ ) in the MFS group (mean  $\pm$  SD,  $-1.1 \pm 2.2$ ) compared with the control group ( $-0.25 \pm 1.5$ ). Indeed, several patients with myopia were referred by ophthalmologists to the Marfan clinic, to explore a suspected phenotype of MFS, and therefore the control group had a lower refractive power than in the general population.

In the systematic biomicroscopic examination, ectopia lentis was observed in 86.7% (52 eyes) of the MFS group and was found in no eyes in the control group (significant difference between the two groups,  $P < 0.0001$ ). Most often, lens dislocation occurred in the superotemporal and the superior area.

### Orbscan Data

All Orbscan data are summarized in Tables 3, 4, and 5 and Figures 1 and 2. Mean K in the 3.0-mm central zone in the MFS group was  $40.8 \pm 1.4$  D (range, 37.5–43.9) and was significantly decreased compared with the control group ( $P < 0.0001$  for both groups), which was  $42.8 \pm 1.0$  D (range, 40.5–44.8). The proportion of flattened corneas (mean K  $< 41.5$  D) determined with the Orbscan system (and the autorefractometer) was significantly higher ( $P < 0.0001$ ) in the MFS group (75.4%; 43/57 eyes) than in the control group (12.5%; 4/32 eyes). Moreover, patients with MFS and presence of ectopia lentis had mean K of  $40.8 \pm 1.5$  D, ranging from 37.5 to 43.9 D. Sim K measures in the MFS group (Fig. 1) were  $40.8 \pm 1.4$  D (range, 37.5–43.9) versus  $42.9 \pm 1.1$  D (range, 40.4–44.9) for the control group ( $P < 0.0001$ ).

Control group mean A in the 3.0-mm central zone was  $0.78 \pm 0.47$  D (range, 0.1–2.0) which was not significantly different from that in the MFS group (mean A,  $1.09 \pm 0.87$  D; range, 0.1–4.9,  $P = 0.06$ ). However, MFS group mean sim A ( $1.07 \pm 0.84$  D; range, 0.1–5.2) was significantly decreased ( $P = 0.03$ ) compared with the control group ( $0.72 \pm 0.43$  D; range, 0.1–1.7).

An Orbscan pachymetry example is represented in Figure 3 showing a pachymetric pattern of central thickness, and 10 midperipheral locations, in a patient with MFS; four data points were important to us in the study: central thickness, eight midperipheral thicknesses, thinnest corneal point measurement, and type of pattern. These data are summarized in Tables 3, 4, and 5. Central thickness in the MFS group was  $502 \pm 41.9$   $\mu$ m (range, 429–606), significantly lower than in the control group ( $552.4 \pm 23.6$   $\mu$ m; range, 510–609;  $P < 0.0001$ ). In the MFS group, 34 (56.7%) of 60 eyes had a central thickness below 520  $\mu$ m, whereas only 2 (6.2%) of 32 eyes in the control group showed a statistical difference ( $P < 0.0001$ ). In the same way, the thinnest corneal point measured in the MFS group was  $487.2 \pm 42.2$   $\mu$ m, ranging from 412 to 585  $\mu$ m versus  $542.2 \pm 25$   $\mu$ m (range, 496–598) for the control group ( $P < 0.0001$ ). In Table 4, central and eight midperipheral location pachymetry measurements (mean  $\pm$  SD) are summarized. In the central, superotemporal, nasal, superonasal, and superior areas, pachymetric measurements were significantly lower in the MFS group than in the control group ( $P < 0.0001$ ). In temporal, inferotemporal, inferior, and inferonasal areas, there was the same difference (respective probabilities were 0.005, 0.04, 0.002, and 0.0007). Each time, in both groups, among the nine regions evaluated, the central cornea was found to be the thinnest ( $502 \pm 42$   $\mu$ m in the MFS group and  $552 \pm 24$   $\mu$ m in the control group).

In Table 5, in the MFS group as in the control group, the preferential location of the thinnest corneal site was the inferotemporal quadrant (respectively, 55% and 62.6%). The principal data were the higher proportion of location in the inferonasal quadrant in the MFS group (16.4%, versus 6.2% in the control group). The thinnest corneal site distance from the visual axis was barely higher in the MFS group (0.92 mm) than in the control group (0.82 mm). Pachymetry color-coded maps were classified into round, oval, decentered round, and decentered oval patterns. In the control group, the majority of eyes had either oval (50%) or round (43.7%) patterns, whereas the MFS group had more round (58.3%) than oval (38.3%) patterns ( $P = 0.59$ ).

TABLE 4. Orbscan Corneal Thickness in Each Location

	Central	Supero Temporal	Temporal	Infero Temporal	Inferior	Infero Nasal	Nasal	Supero Nasal	Superior
MFS	502 $\pm$ 42	563 $\pm$ 40	566 $\pm$ 45	576 $\pm$ 47	584 $\pm$ 44	594 $\pm$ 46	587 $\pm$ 40	576 $\pm$ 44	573 $\pm$ 47
Control	552 $\pm$ 24	603 $\pm$ 27	592 $\pm$ 28	595 $\pm$ 29	613 $\pm$ 30	627 $\pm$ 30	626 $\pm$ 30	631 $\pm$ 30	635 $\pm$ 24
<i>P</i>	<0.0001	<0.0001	0.005	0.04	0.002	0.0007	<0.0001	<0.0001	<0.0001
Liu et al. <sup>8</sup>	560 $\pm$ 30	620 $\pm$ 30	590 $\pm$ 30	600 $\pm$ 30	630 $\pm$ 30	630 $\pm$ 30	610 $\pm$ 30	630 $\pm$ 30	640 $\pm$ 30
Dursun et al. <sup>11</sup>	558 $\pm$ 18	621 $\pm$ 26	589 $\pm$ 17	609 $\pm$ 17	632 $\pm$ 22	626 $\pm$ 22	614 $\pm$ 16	638 $\pm$ 14	653 $\pm$ 18

Data are expressed as mean micrometers  $\pm$  SD. Probabilities are MFS versus control.

**TABLE 5.** Location of the Thinnest Corneal Point Measured by the Orbscan and the Average Pachymetric Pattern

	Marfan	Control	Liu et al. <sup>8</sup>
Location of the thinnest corneal point			
Inferotemporal Quadrant (%)	55.0	62.6	69.57
Superotemporal Quadrant (%)	26.8	28.1	23.91
Inferonasal Quadrant (%)	16.4	6.2	4.35
Superonasal Quadrant (%)	1.8	3.1	2.17
Distance from the corneal center (mm)	0.92	0.82	0.90
Average pachymetric pattern			
Round (%)	53.3	43.7	41.30
Oval (%)	38.3	50.0	47.83
Decentred round (%)	3.4	0.0	2.18
Decentred oval (%)	5.0	6.3	8.70

### In Vivo Confocal Microscopy

MFS keratocyte nuclei were embedded in an opaque stromal matrix but morphology and density were normal. Stromal and corneal thicknesses were thinner in every case, and Z-scan profiles were abnormal with an increased back scattering of light in the stroma, with blurred images. Indeed, as seen in Figure 4, the stromal level of reflectivity was normally lower than those in the epithelium and endothelium. However, in the Marfan cornea, the increased back scattering of light induced a higher level of the stromal plateau in comparison with epithelium and endothelium reflectivities, which were smoothed down. Mean reflectivity obtained in the 14 Marfan corneas measured was statistically higher than in the 14 normal corneas ( $0.61 \pm 0.073$  vs.  $0.48 \pm 0.068$ ,  $P = 0.009$ ).

Epithelial and endothelial cells appeared to be regular in shape, and the subbasal nerves were visible and comparable to those of a normal cornea.

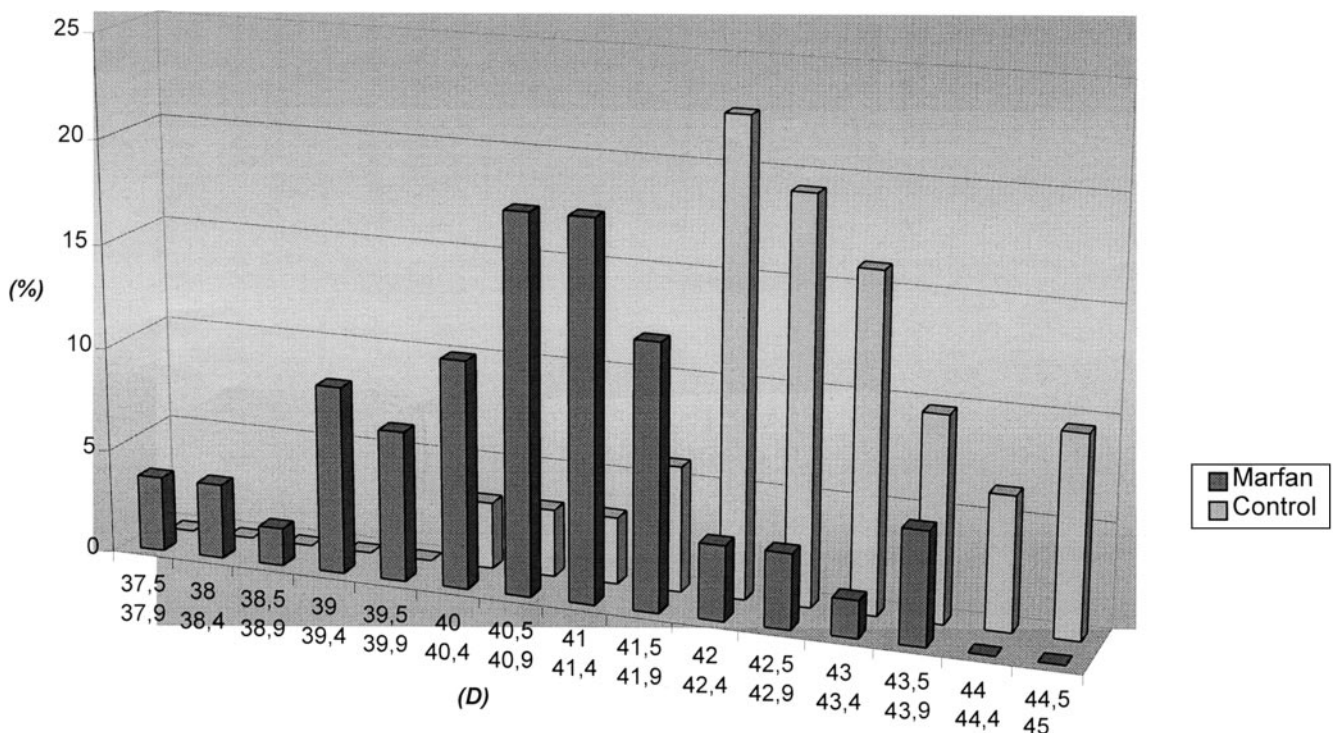
### Correlation Analyses

All data are summarized in Table 6. First, as expected, autorefractometer and Orbscan mean keratometries in the 3.0-mm central zone showed strong positive correlation ( $P < 0.0001$ ). In the same way, Orbscan mean K correlated positively with sim K ( $P < 0.0001$ ). In Table 7, keratometry and pachymetry were established in the group of patients with ectopia lentis. In comparison with other patients, significant differences were described. The presence of ectopia lentis was linked with decreased pachymetry (central,  $483.7 \pm 36.4 \mu\text{m}$  in the group with dislocation of the lens versus  $547.2 \pm 32.1$  in the group without;  $P < 0.0001$ ), keratometry (mean K,  $41.3 \pm 1.3$  D in the group with dislocation of the lens versus  $42.7 \pm 1.1$  D in the group without), and conversely. There was no statistical correlation between corneal thickness and refractive power ( $P = 0.12$ ). Finally, neither central nor thinnest pachymetries correlated significantly with mean K or sim K.

### DISCUSSION

In this study, an MFS-affected cornea was confirmed to be flattened. These data, well known for 20 years, are included in the Berlin criteria<sup>2</sup> and in the revised diagnostic criteria for MFS,<sup>9</sup> as a minor sign. In autorefractometer mean K data, we obtained results comparable to those of Maumenee<sup>10</sup> in her MFS group (mean K,  $41.38 \pm 2.04$  D) and to other mean corneal powers of normal eye (range, 43.0–44.0). Control group mean A in the 3.0-mm central zone ( $0.78 \pm 1.4$  D) was not significantly different from that of the MFS group ( $1.09 \pm 0.87$  D). Maumenee<sup>10,12</sup> reported a mean A of  $1.47 \pm 1.51$  D, but 33.4% of the eyes had a cylinder of less than 0.5 D.

Moreover, with Orbscan pachymetry, MFS-affected corneas appeared to be significantly thinner in the central ( $502 \pm 41.9 \mu\text{m}$ ) and peripheral areas than corneas of normal eyes ( $552 \pm 23.6 \mu\text{m}$ ), which has not been described in the literature. In 1981, Maumenee<sup>10</sup> reported pachymetry measurements in 11

**FIGURE 1.** Orbscan sim K measurement in the two groups.

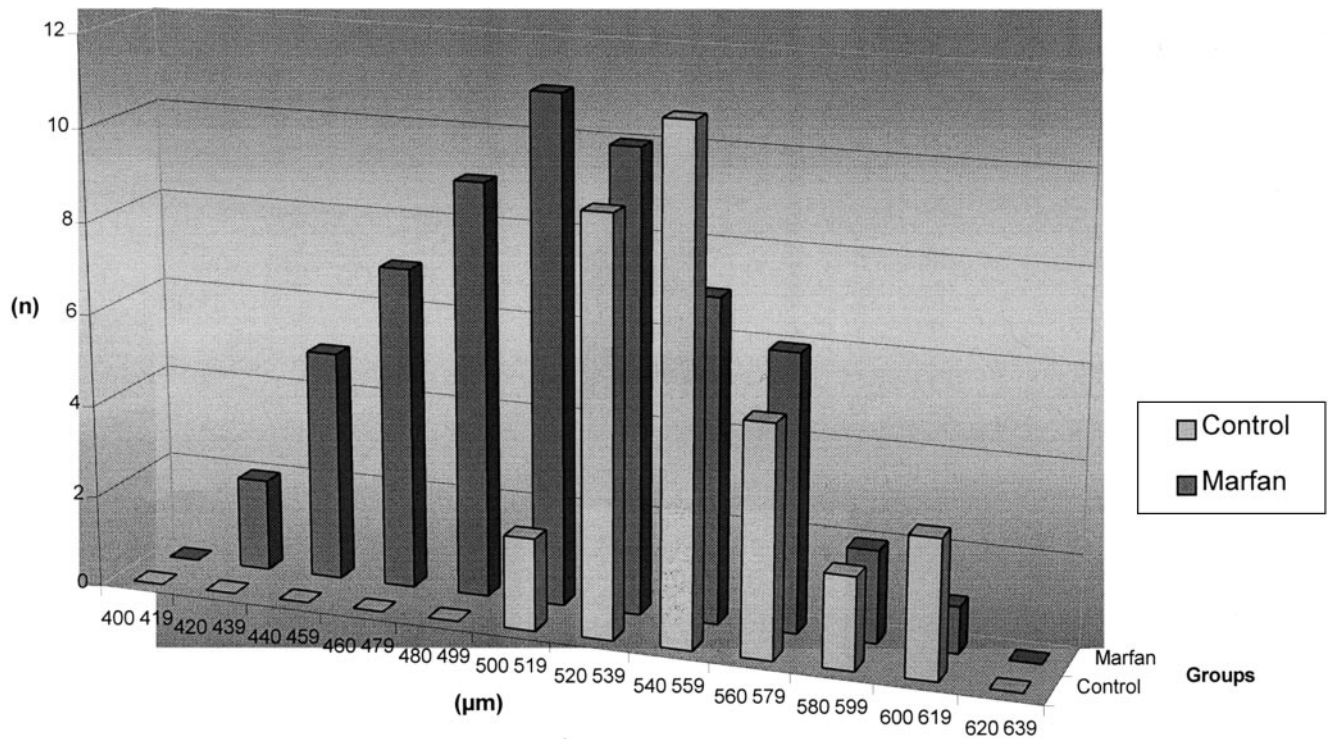


FIGURE 2. Orbscan central pachymetry measurements in the two groups.

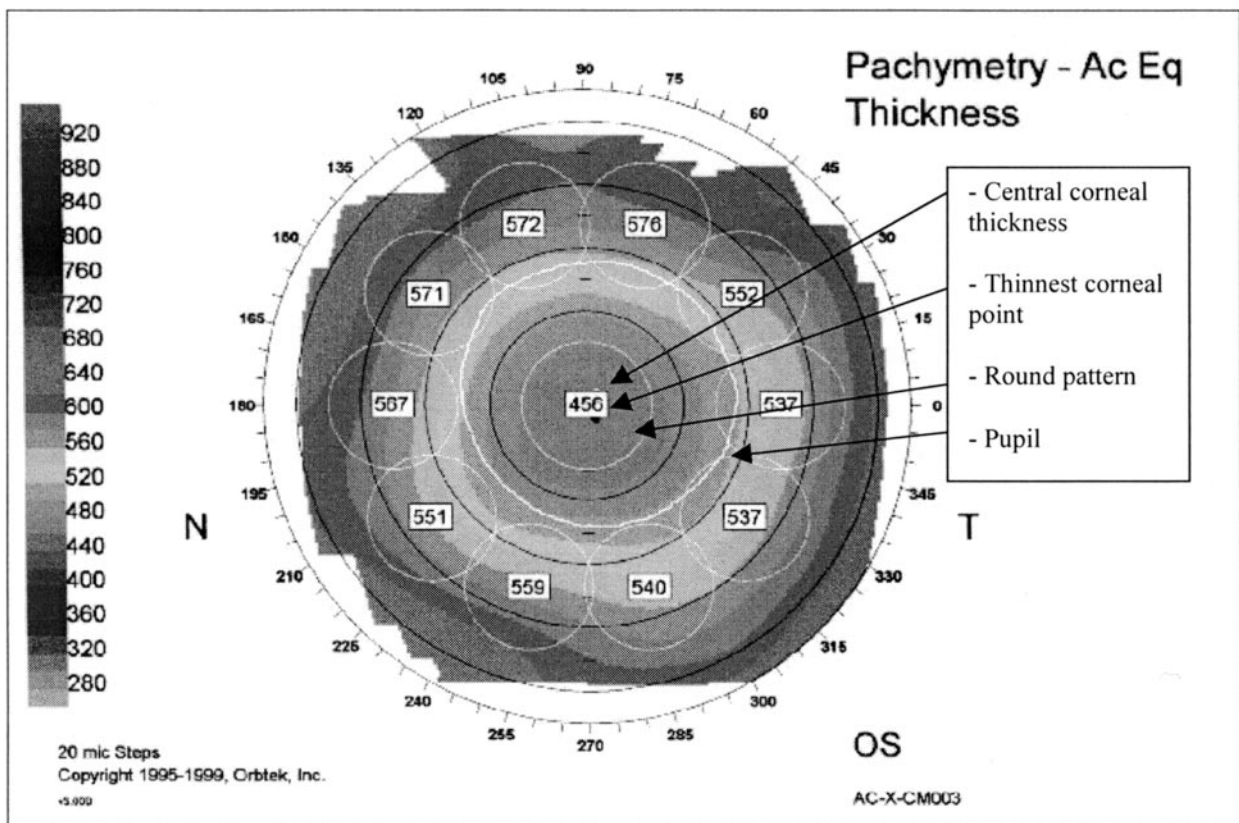
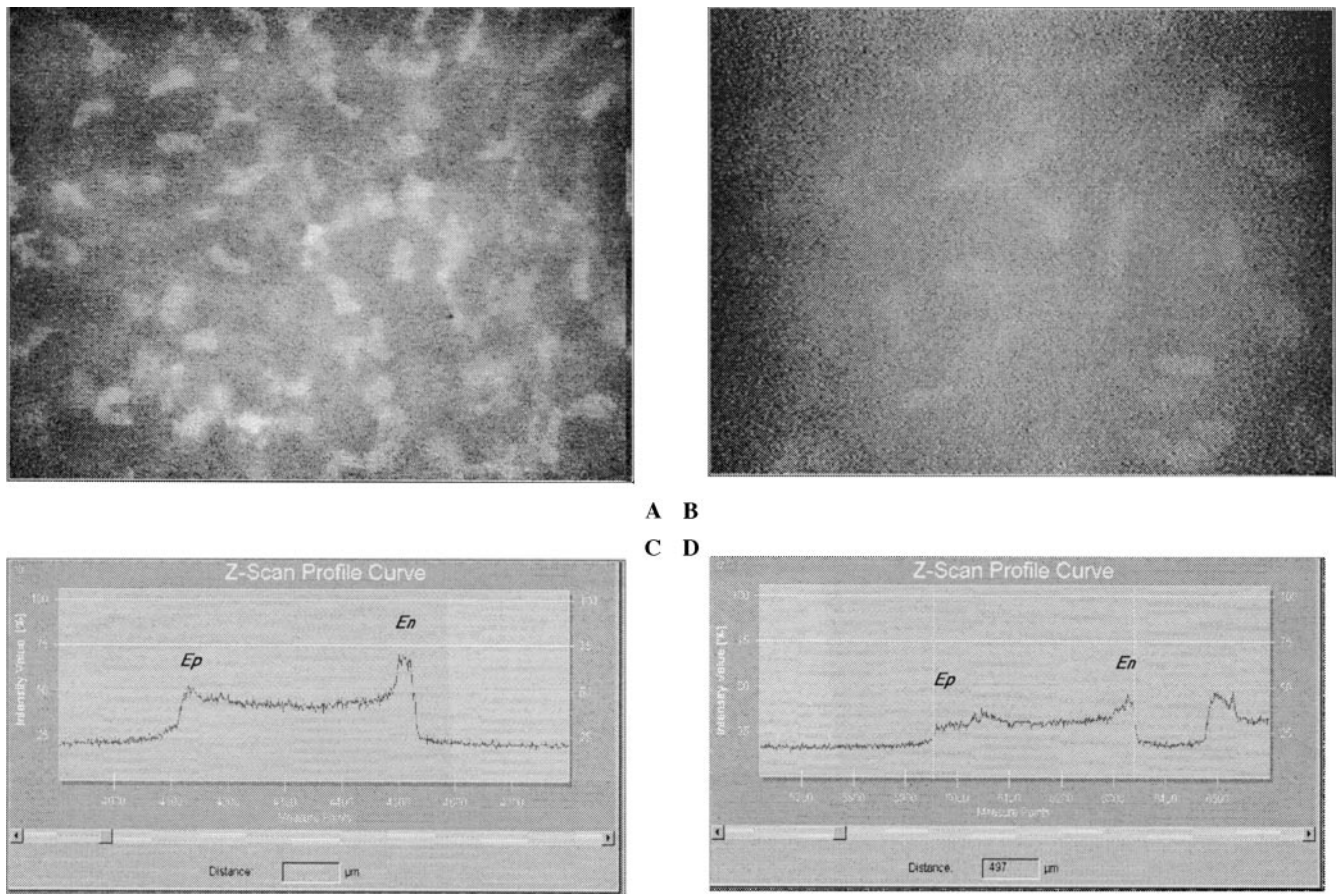


FIGURE 3. This example of a pachymetric pattern (central and 10 midperipheral locations) generated with the Orbscan system, in a patient with MFS, shows a central corneal thickness of 256 µm, a thinnest corneal point in the temporal inferior quadrant of 450 µm, and a centered round pattern.



**FIGURE 4.** In vivo confocal microscopy (A, B). The Z-scan profile curve (C, D) confirms corneal thinning with stromal hyperreactivity in the MFS-affected cornea (D) and shows an opaque extracellular matrix (B), as can be seen by loss of epithelial (Ep) and endothelial (En) peaks. (A) and (C) represent a normal cornea.

patients, but did not notice any statistical difference with the normal population. In our control group, pachymetry measurements were close to those of Liu et al.<sup>8</sup> and Dursun et al.,<sup>11</sup> for normal eyes. Indeed, in these three groups of normal eyes, superior and superonasal regions were always the thickest (in our study, respectively,  $635 \pm 24$  and  $631 \pm 30 \mu\text{m}$ ), and inferotemporal, temporal, and central regions were always the thinnest (in our study, respectively,  $595 \pm 29$ ,  $592 \pm 28$ , and  $552 \pm 24 \mu\text{m}$ ). In our MFS group, it is important to note that results were almost inverse: The central pachymetry remained

the thinnest ( $502 \pm 24 \mu\text{m}$ ), but the thickest corneal regions were (in order of decreasing thickness) inferonasal, nasal, inferior, and inferotemporal (respectively,  $594 \pm 46$ ,  $587 \pm 40$ ,  $584 \pm 44$ , and  $576 \pm 47 \mu\text{m}$ ), whereas the thinnest regions were (in the same order) superonasal, superior, temporal, superotemporal, and central areas (respectively,  $576 \pm 44$ ,  $573 \pm 47$ ,  $566 \pm 45$ ,  $563 \pm 40$ , and  $502 \pm 24 \mu\text{m}$ ). Therefore, in Marfan disease, the whole cornea was significantly thinner than in the normal eye, and traditional variations in corneal thickness were different. In normal eyes, the superior area was always thicker than the inferior one, which was the opposite in Marfan corneas.

The ocular enlargement was known to be a common, if not invariable, feature of MFS,<sup>13</sup> followed later by the scleral thin-

**TABLE 6.** Correlations of Clinical and Orbscan Corneal Topography System Data

	Correlation Coefficient	P
Mean K, mean K (AR*)	0.93	<0.0001
Mean K, sim K	0.98	<0.0001
Mean K, central pachymetry	-0.27	NS
Mean K, thinnest pachymetry	-0.27	NS
Mean K, refractive power	0.24	0.05
Sim K, central pachymetry	-0.14	NS
Sim K, thinnest pachymetry	-0.15	NS
Sim K, refractive power	0.26	0.02
Central pachymetry, thinnest pachymetry	0.97	<0.0001
Central pachymetry, refractive power	0.21	NS
Thinnest pachymetry, refractive power	0.2	NS

\* Autorefractometer data.

**TABLE 7.** Comparison of Measurements between Patients with and Those without Ectopia Lentis

	No Ectopia Lentis	P*	Ectopia Lentis
Mean K (D)	$42.7 \pm 1.1$	<0.0001	$41.3 \pm 1.3$
Sim K (D)	$42.8 \pm 1.1$	<0.0001	$41.3 \pm 1.3$
Central thickness ( $\mu\text{m}$ )	$547.2 \pm 32.1$	<0.0001	$483.7 \pm 36.4$
Thinnest corneal point ( $\mu\text{m}$ )	$536.7 \pm 32.6$	<0.0001	$469.7 \pm 38.1$
Refractive power (D)	$-0.25 \pm 1.7$	NS	$-1.25 \pm 2.3$

Data are the mean  $\pm$  SD.

\* Compared with control.

ness; the degree of enlargement is not uniform, and there could be an exaggeration of the corneal scleral groove. The following question then occurs: Are sclera and cornea thin because of ocular enlargement, or do the histologic abnormalities of Marfan disease generate thinness and change their consistency?

Fibrillin is widely distributed throughout ocular tissues and participates in an extensive elastic fiber system.<sup>13-15</sup> It has been observed in human and bovine cornea with variable patterns of location. Wheatley et al.<sup>13</sup> detected only patchy traces of fibrillin in normal corneal stroma, localized in spaces between the collagen lamellae. Fibrillin is present in newborn, but not adult, corneas.<sup>16</sup> Pessier and Potter<sup>17</sup> suggested abnormal deposition of fibrillin in the extracellular matrix (ECM). The epithelial basement membrane region consistently exhibits fibrillin staining, particularly in the peripheral cornea, where a dense band of staining is present between the corneal epithelium and Bowman's layer, but was faint in the central cornea.<sup>13,18</sup> This pattern could be related to an increased hemidesmosome content in the epithelial basement membrane zone when moving from limbus to central cornea. No staining of the Descemet membrane or the corneal endothelium was detected. In addition, fibrillin was detected in pathologic corneas, such as in bullous keratopathy,<sup>19</sup> after refractive surgery,<sup>20,21</sup> and in keratoconus.<sup>22</sup> It has been proposed that cornea flattening in Marfan is due to the increased dimension of the whole globe. Products of an altered fibrillin gene could be responsible for a thin peripheral cornea, because of the dense band of fibrillin that exists between the corneal epithelium and Bowman's layer. Then, because of the eye enlargement, the whole globe could be "stretched" over time, with, essentially, thin cornea (even in the center) and other ocular tissues.

Fibrillin-1 is a major component of the 10- to 12-nm microfibrils that are thought to play a role in tropoelastin deposition and elastic fiber formation and to possess an anchoring function.<sup>23</sup> In the cornea, the microfibrils may act as a flexible mechanical anchor at epithelial-mesenchymal basement membrane interfaces, as is found in the dermal-epidermal junction. Morphologic abnormalities of elastic components contribute to centrifugal stretching of the cornea and the sclera. Intraocular pressure can then generate ocular enlargement. In this way, the more stretched the eye, the thinner and more flattened the sclera and cornea, and the final stage may be megalocornea or cornea plana.

In our MFS group, we found that keratometry and pachymetry were both highly associated with ectopia lentis ( $P < 0.0001$ ). Thus, morphologic abnormalities resulting from mutations in fibrillin-1 produced the same flattening and thinning of the cornea and dislocation of the lens. Examination of ocular tissues of patients with MFS with ectopia lentis revealed zonular fibers reduced in number,<sup>24-26</sup> thin, stretched, irregular in diameter,<sup>16</sup> inelastic, and easily broken when compared with normal control subjects.

Despite the abnormal thinning of cornea in the MFS group, neither keratoconus nor corneal ectasia was detected, even with Orbscan posterior elevation and topography. Comparable results were obtained by Maumenee,<sup>10,12</sup> who did not observe any keratoconus in her series of 160 patients with MFS. Nevertheless, Kenney et al.<sup>22</sup> found that fibrillin-1 was expressed in keratoconus corneas but was absent in all normal central corneas and was seen only in the normal limbus and the conjunctiva (in agreement with most previous data).

The Orbscan corneal topography system is a device developed to evaluate anterior and posterior corneal surface topography and thickness of the entire cornea. Orbscan pachymetry is obtained using a 3-D scanning optical slit device (an advantage is that it is a noncontact method), which can detect small

hydration-based, transient, corneal thickness fluxes. According to Lattimore et al.,<sup>6</sup> the accuracy and variability (precision) of pachymetry measurements using the Orbscan system is acceptable for use in research.<sup>6,7,27</sup>

Yaylali et al.<sup>28</sup> reported that the relative accuracy and precision of this system was similar to those of ultrasonic pachymetry, although they found that thickness measurements were 23 to 28  $\mu\text{m}$  greater than those obtained by ultrasonic pachymetry (but always separated by the same difference). In addition to that, pachymetric measurements of central thickness made in the Prospective Evaluation of Radial Keratotomy (PERK)<sup>8</sup> study were 20  $\mu\text{m}$  thinner than the measurements obtained with the Orbscan system, and 54  $\mu\text{m}$  for Marsich and Bullimore.<sup>7</sup> In our control group, results showed that central pachymetry (552  $\mu\text{m}$ ) was similar to many previous data, but some midperipheral measurements appeared to be thinner. However, pachymetry measurements were performed with the same system in our two groups.

In vivo confocal microscopy in 14 corneas of patients with MFS confirmed corneal thinning, depending on the stroma, with an opaque stromal matrix (Fig. 4). Z-scan profiles were abnormal with an increased stromal back scattering of light (Fig. 4). These last data were observed in cornea plana,<sup>29</sup> which can be considered a different entity, with genetic transmission (an autosomal recessive mode of inheritance), because in the cornea of patients with MFS, Vesaluoma et al.<sup>29</sup> found that midstromal keratocyte nuclei were embedded in an opaque matrix and that posterior keratocyte nuclei were obscured, due to opaqueness of the stromal matrix. Even with substantial flattening of the cornea, however, confocal microscopic abnormalities of MFS are not the same as in cornea plana, in which stromal and total thicknesses are close to normal, with a reduced epithelial layer. Moreover, the Bowman layer is absent, and subbasal nerves have abnormal branching patterns, contrary to that observed in MFS, suggesting the role of fibrillin location in the epithelial layer of the corneal periphery.

In conclusion, because positive diagnosis of MFS is still difficult, ophthalmologists treating this disease need help, particularly in cases of minor ectopia lentis. Minor signs, such as flattened corneas, are very useful. In line with our findings on the cornea in MFS, in our Marfan clinic, we offer systematic pachymetry to patients with suspected MFS, tracking a thin cornea, highly significantly associated with ectopia lentis. Moreover, normal intraocular pressure associated with a thin cornea, may lead to suspicion of authentic chronic glaucoma, appearing as a possible complication of MFS, almost simultaneously with ectopia lentis. This easily detectable sign could be considered a new minor sign of MFS. It would be of interest to perform further investigations to confirm these findings and elucidate the mechanisms.

## APPENDIX

### Marfan Study Group

Catherine Boileau, Sylvie Molcard, Florence Tubach, Jean-Marie Leparç, Christine Muti, Bertrand Chevalier, and Guillaume Jondeau, from the Marfan Clinic of Ambroise Pare Hospital, University of Paris-V, Paris, France.

### References

1. Robinson PN, Godfrey M. The molecular genetics of Marfan syndrome and related microfibrillinopathies. *J Med Genet.* 2000;37:9-25.
2. Sakai LY, Keene DR, Engvall E. Fibrillin, a new 350-kD glycoprotein, is a component of extracellular microfibrils. *J Cell Biol.* 1986;103:2499-2509.

3. Ramirez F, Lee B, Vitale E. Clinical and genetic associations in Marfan syndrome and related disorders. *Mt Sinai J Med.* 1992;59:350-356.
4. Chikumi H, Yamamoto T, Ohta Y, et al. Fibrillin gene (FBN1) mutations in Japanese patients with Marfan syndrome. *J Hum Genet.* 2000;45:115-118.
5. Beighton P, De Paepe A, Danks D, et al. International nosology of heritable disorders of connective tissue, Berlin. *Am J Med Genet.* 1988;29:581-594.
6. Lattimore MR Jr, Kaupp S, Schallhorn S, Lewis R. Orbiscan pachymetry: implications of a repeated measures and diurnal variation analysis. *Ophthalmology.* 1999;106:977-981.
7. Marsich MW, Bullimore MA. The repeatability of corneal thickness measures. *Cornea.* 2000;19:792-795.
8. Liu Z, Huang AJ, Pflugfelder SC. Evaluation of corneal thickness and topography in normal eyes using the Orbscan corneal topography system. *Br J Ophthalmol.* 1999;83:774-778.
9. De Paepe A, Devereux RB, Dietz HC, Hennekam R, Pyeritz RE. Revised diagnostic criteria for the Marfan syndrome. *Am J Med Genet.* 1996;62:417-426.
10. Maumenee IH. The eye in the Marfan syndrome. *Trans Am Ophthalmol Soc.* 1981;79:684-733.
11. Dursun D, Monroy D, Knighton R, et al. The effects of experimental tear film removal on corneal surface regularity and barrier function. *Ophthalmology.* 2000;107:1754-1760.
12. Maumenee IH. The cornea in connective tissue diseases. *Ophthalmology.* 1978;85:1014-1017.
13. Wheatley HM, Traboulsi EI, Flowers BE, et al. Immunohistochemical localization of fibrillin in human ocular tissues. *Arch Ophthalmol.* 1995;113:103-109.
14. Streeten BW, Licari PA, Marucci AA, Dougherty RM. Immunohistochemical comparison of ocular zonules and the microfibrils of elastic tissue. *Invest Ophthalmol Vis Sci.* 1981;21:130-135.
15. Ashworth JL, Kielty CM, McLeod D. Fibrillin and the eye. *Br J Ophthalmol.* 2000;84:1312-1317.
16. Zaidi TS, Hasan A, Baum J, Panjwani N. Localization of fibrillin in normal human and bovine corneas [ARVO Abstract]. *Invest Ophthalmol Vis Sci.* 1991;32(4):S875. Abstract nr 1017.
17. Pessier AP, Potter KA. Ocular pathology in bovine Marfan's syndrome with demonstration of altered fibrillin immunoreactivity in explanted ciliary body cells. *Lab Invest.* 1996;75:87-95.
18. Raghunath M, Cankay R, Kubitscheck U, et al. Transglutaminase activity in the eye: cross-linking in epithelia and connective tissue structures. *Invest Ophthalmol Vis Sci.* 1999;40:2780-2787.
19. Ljubimov AV, Saghizadeh M, Spirin KS, Mecham RP, Sakai LY, Kenney MC. Increased expression of fibrillin-1 in human corneas with bullous keratopathy. *Cornea.* 1998;17:309-314.
20. Ljubimov AV, Alba SA, Burgeson RE, et al. Extracellular matrix changes in human corneas after radial keratotomy. *Exp Eye Res.* 1998;67:265-272.
21. Maguen E, Alba SA, Burgeson RE, et al. Alterations of corneal extracellular matrix after multiple refractive procedures: a clinical and immunohistochemical study. *Cornea.* 1997;16:675-682.
22. Kenney MC, Nesburn AB, Burgeson RE, Butkowsky RJ, Ljubimov AV. Abnormalities of the extracellular matrix in keratoconus corneas. *Cornea.* 1997;16:345-351.
23. Kielty CM, Davies SJ, Phillips JE, Jones CJP, Shuttleworth CA, Charles SJ. Marfan syndrome: fibrillin expression and microfibrillar abnormalities in a family with predominant ocular defects. *J Med Genet.* 1995;32:1-6.
24. Traboulsi EI, Whittum-Hudson JA, Mir SH, Maumenee IH. Microfibril abnormalities of the lens capsule in patients with Marfan syndrome and ectopia lentis. *Ophthalmic Genet.* 2000;21:9-15.
25. Ramsey MS, Fine BS, Shields JA, Yanoff M. The Marfan syndrome. A histopathologic study of ocular findings. *Am J Ophthalmol.* 1973;76:102-116.
26. Mir S, Wheatley HM, Maumenee-Hussels IE, et al. A comparative histologic study of the fibrillin microfibrillar system in the lens capsule of normal subjects and subjects with Marfan syndrome. *Invest Ophthalmol Vis Sci.* 1998;39:84-93.
27. Auffarth GU, Tetz MR, Biazid Y, Volcker HE. Measuring anterior chamber depth with the Orbscan Topography System. *J Cataract Refract Surg.* 1997;23:1351-1355.
28. Yaylali V, Kaufman SC, Thompson HW. Corneal thickness measurements with the Orbscan Topography System and ultrasonic pachymetry. *J Cataract Refract Surg.* 1997;23:1345-1350.
29. Vesaluoma MH, Sankila EM, Gallar J, et al. Autosomal recessive cornea plana: in vivo corneal morphology and corneal sensitivity. *Invest Ophthalmol Vis Sci.* 2000;41:2120-2126.